



Audio Engineering Society Convention Paper 5886

Presented at the 115th Convention
2003 October 10–13 New York, New York

This convention paper has been reproduced from the author's advance manuscript, without editing, corrections, or consideration by the Review Board. The AES takes no responsibility for the contents. Additional papers may be obtained by sending request and remittance to Audio Engineering Society, 60 East 42nd Street, New York, New York 10165-2520, USA; also see www.aes.org. All rights reserved. Reproduction of this paper, or any portion thereof, is not permitted without direct permission from the Journal of the Audio Engineering Society.

The Development of a Forward Radiating Compression Driver by the Application of Acoustic, Magnetic and Thermal Finite Element Methods

Mark Dodd
Celestion Int. Ltd. Ipswich, Suffolk, United Kingdom.

ABSTRACT

A compression driver with an annular two-slot phase-plug coupled to the convex side of a hemispherical diaphragm is introduced. Magnetic and thermal domains are modelled using transient and static Finite Element Methods (FEM). Structural and acoustic domains are modelled as finite elements with boundary elements used to model free space. Structural and acoustic elements are fully coupled to both each other and the boundary elements.

The application of these FEM techniques to the optimisation of compression driver performance is discussed and illustrated with results. The limitations of plane-wave tube measurements are also mentioned and illustrated with FEM and measured results.

1. INTRODUCTION

This paper is about the development of a compression driver, during which a variety of FEM techniques were applied to help optimise the design in respect to its acoustic, magnetic and thermal behaviour. In previous work, fully coupled vibro-acoustic BEM/FEM has been used to simulate the constant force response of a driver, and magneto-static FEM has been used to calculate magnetic flux in the gap [1]. In more recent work transient

magnetic analysis has been used to predict coil motion while taking eddy currents into account. Thermal FEM models have also been investigated but they need experimental data to give accurate results.

The ideal FEM software for loudspeaker design would provide full coupling between magnetic, structural, acoustic, and thermal FEM models together with electrical circuits. However, to the author's knowledge, such a system does not exist and

furthermore if it did, the full coupling would result in very long solution times making the model unwieldy. In this paper, a new approach has been used in which a one-dimensional coupling between magnetic and vibro-acoustic FEM results has allowed the simulation of a driver response driven by a voltage source. Thermal FEM has been applied as a separate analysis to provide qualitative results to aid material choice.

2. THE DRIVER

The aim of the work described in this paper was to produce an economic compression driver with a one-inch diameter throat capable of producing maximum SPL with low distortion over an extended bandwidth. It was also a requirement that the unit should be easy to crossover and should couple to practical horns, giving good dispersion at higher frequencies.

The most recent versions of front loaded compression drivers use a one-inch voice coil to drive a PETP diaphragm loaded by a single slot phase-plug (Mylar and Melinex are well known trade names of PolyEthyleneTetraPhalate, PETP). Magnetic fluid cannot be used to aid coil cooling, however, since it damps the mechanical resonances used to extend the high frequency bandwidth, negating the thermal benefits of the fluid. Compared to conventional 'one inch' compression drivers, these drivers are very economic to manufacture, but handle relatively low power and must be used with a high crossover frequency.

Our requirements for extended bandwidth and high maximum SPL point to the use of a larger diaphragm and voice coil. Rather than extending the high frequency bandwidth by means of structural resonances, it was decided to try and keep the structure moving as a rigid body within the working range. After some initial analysis, a 34mm diameter deep drawn aluminium dome with voice coil wound directly on the dome skirt was chosen. This dome is supported by a 1mm wide elastomer suspension to allow large excursions without failure due to fatigue. This moving structure is sufficiently rigid for magnetic fluid to be added to the gap with little effect to the frequency response.

Unsuppressed Bessel-type cavity modes between phase-plug and diaphragm result in severe response dips; these dips are both deep and wide. The larger diameter diaphragm chosen here places both the first and second order cavity modes in our bandwidth. Suppressing these two modes requires a two-slot phase-plug [3]. It is a major limitation of 'front

loading' that the phase-plug must either have only a single slot or face the difficulty of having to produce an acoustic delay in one or more slots to correct the path-length differences. As we shall see later in the paper, the exact shape of these slots must be chosen to produce the desired wavefront shape at the driver exit.

3. COMPRESSION DRIVER TERMINATION

Compression drivers are inevitably used with some type of horn. The response without a horn is of little practical value, although in the past it has been used to validate modelling results [1][2]. Since both horn throat impedance and dispersion vary strongly between individual horn designs, it is common practice to use a plane-wave tube in an attempt to evaluate the driver performance loaded with an acoustic resistance. However, while compression drivers are often intended to produce plane waves, this limits the high frequency dispersion. The new driver is designed to produce a spherical cap with a 25 degree included angle to give good dispersion in a wide variety of practical horns. When coupled to a plane-wave tube, this wave-front shape will result in cross-modes being excited above the cut off frequency of the plane-wave tube.

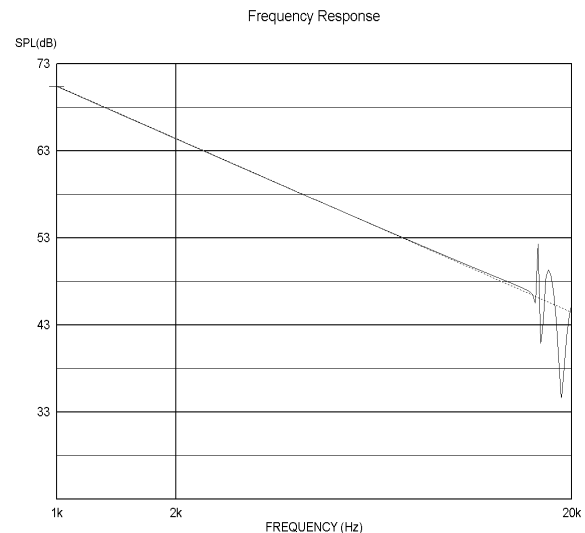


Figure 1
SPL for planar and pulsating Spherical waves 0.1m
down plane-wave tube

However, the plane-wave tube is ideal for examining the low frequency lumped element behaviour, so we decided to investigate the limitations of this method when used with a non-planar source. To this end, two FEM models were made of an infinite tube driven firstly by a planar source and secondly by a pulsating spherical source. In both cases, the source

is defined to have constant amplitude sinusoidal volume-acceleration, equivalent to applying a constant driving force with a mass load. The modelled tube is terminated by coupling the FEM region with a series solution obtained using the separability of the Helmholtz equation in cylindrical coordinates [4]. SPL data was extracted at a node 0.1m from the source as in a real plane-wave tube, and this data is shown in Figure 1. As we can see, the pulsating sphere excites modes above 15kHz giving strong peaks and dips in the response curve. The wavefront shapes at 20kHz are shown in Figure 3 for both source types. The plane source produces plane waves at all frequencies. The pressure distribution produced by the spherical source is a linear combination of plane waves and radial modes so has a somewhat complex shape.

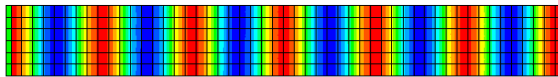


Figure 2.
Shaded pressure plot of sound pressure due to a planar source radiating into an infinite tube

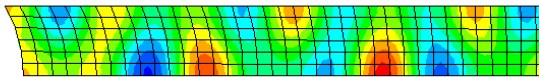


Figure 3
Shaded pressure plot of sound pressure due to a pulsating spherical source radiating into an infinite tube

As a consequence, plane wave tube data must be treated with great caution at frequencies around and above the first cut-off.

4. THE ELECTRO-MAGNETO-VIBRO-ACOUSTICAL FEM METHOD

Vibro-acoustic FEM gives the ability to find the pressure/velocity/displacement at any point in the model. In the frequency range of interest, axial modes of the former are not excited. Hence, it is sufficient to excite with an axial force at a particular position. The mechanical impedance Z_m can be determined as the ratio of the known force and the computed axial velocity. Due to the fully coupled nature of the FEM model, this mechanical impedance

will include radiation and enclosure loading. The transfer function between the displacement at the above position and the SPL at the measurement point are also extracted.

The force arises from the current in the magnetic field. The current can be computed using Z_m and the force factor BL , where B is the mean radial flux and L is the length of wire. The applied voltage can be computed using the blocked voice coil impedance Z_e , but taking account of the back-emf due to coil motion. Using the linearity of the system, the results can be scaled to give a transfer function between input voltage and SPL at the measurement point.

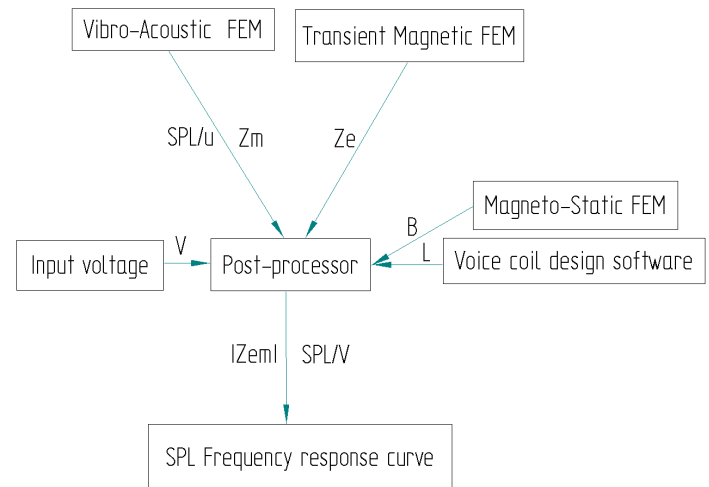


Figure 4
Block diagram of magneto-electrical-vibro-acoustical-model

5. THE APPLICATION OF THE ELECTRO-MAGNETO-VIBRO-ACOUSTICAL FEM METHOD TO COMPRESSION DRIVER DESIGN.

5.1. MAGNETIC ANALYSIS

A parametric model of the magnet was produced using the Flux2D package CEDRAT. The model domain was axisymmetric with second order elements see Figure 5. The model boundary is defined with an 'infinite region' to avoid errors due to modelling only a small region of space [5][6]. This software package allows the problem to be solved over a range of variables defining the geometry. With respect to plate and magnet dimensions, the optimum geometry was selected to obtain the desired static magnetic field. The field in the gap was evaluated over a line of constant radius through the centre of the coil to give B , the average flux density in the gap. The length of wire in the coil

can then be used to calculate BL, the force factor of the coil.

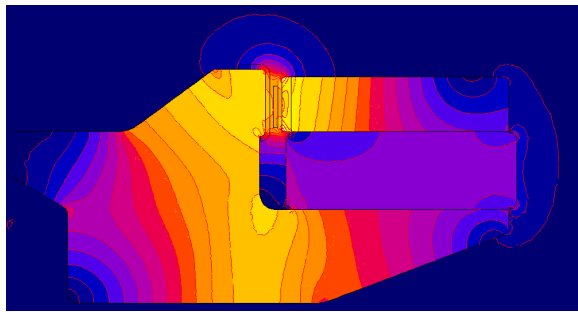


Figure 5

Ring magnet structure used for static and transient analysis. Static lines of constant flux shown

Having obtained the BL, the blocked coil impedance must be calculated. This has been achieved by using Transient Magnetic FEM with the same geometry defining the structure, but re-meshed with a suitable 'skin' of conductive elements, and with a voltage source coupled to the voice coil region [5]. After sufficient time-steps for the starting transient to settle, a steady-state waveform of current versus time may be extracted from the solution files, along with the driving voltage. This analysis includes the effect of eddy currents induced in the pole and the copper sleeve; these may be seen in Figure 6.

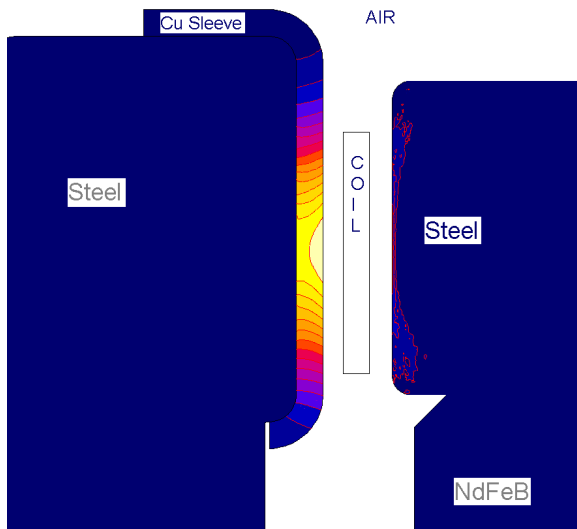


Figure 6

Transient magnetic FEM current density in poles and copper cap for 10,000Hz sinusoidal input. Light indicates high current, dark indicates low current

The current waveform flowing through the coil is

extracted by evaluating the current through the coil at each timestep, a typical result is shown in Figure 7.

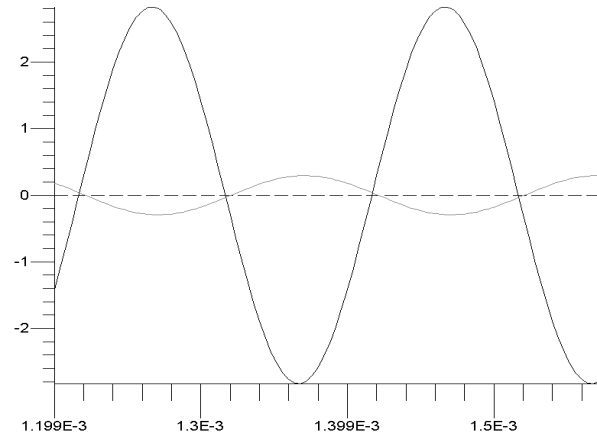


Figure 7

Transient Magnetic FEM output for 5000Hz sinusoidal input 2.8V (black curve) and derived Current through voice coil (grey curve) plotted against time

Subsequently the voice coil's 'blocked' electrical impedance may be calculated by applying Ohm's law. The real and imaginary parts of the example coil are plotted in Figure 8 for a range of frequencies. The four calculated values of blocked coil impedance shown were used to calculate SPL and driver input impedances throughout this paper.

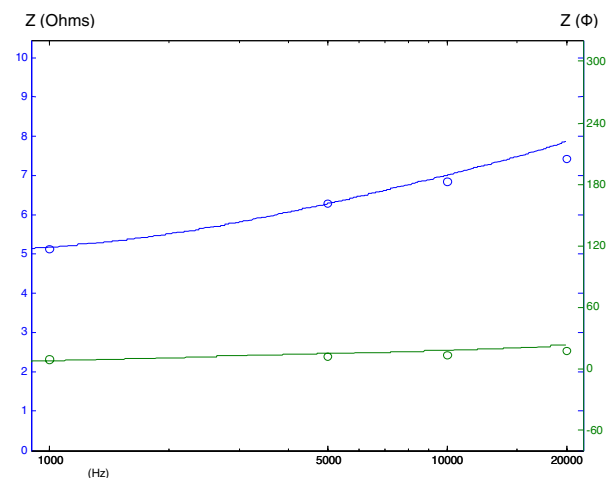


Figure 8

Magnitude (upper curve) and Phase (lower curve) components of voice coil electrical impedance. Solid line measured, circles modelled

6. Vibro-acoustic model

The new compression driver was modelled on a plane-wave tube, terminated by coupling the FEM region with the series solution, obtained using the separability of the Helmholtz equation in cylindrical coordinates. A 2D axisymmetric model domain was used to give best computational speed for the axisymmetric structure. Quadratic elements are used for acoustic and structural regions; they require only three elements per wavelength, unlike the six required by the first order elements described in [7]. An example of the type of mesh used is shown in Figure 9.

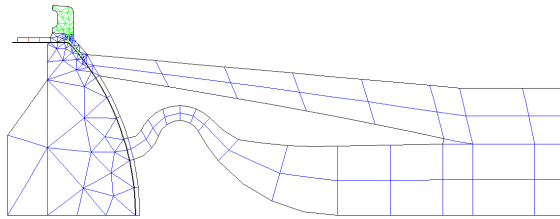


Figure 9

Mesh used for Vibro-Acoustic analysis of driver on plane-wave tube

Initial work with the model was hampered by a lack of data for the rubber suspension used. The results shown in this paper have used values of Young's modulus and loss factor adjusted to give "best fit" to measured data. It was also found necessary to include volume absorption to give the correct modal damping due to the viscous properties of air between the phase-plug and the diaphragm.

The air-cavity in the voice coil gap and within the magnet is neglected in this model due to the presence of ferrofluid in the gap. This avoids the magnet cavity modes found in the 'generic front loaded' benchmark driver which does not use ferrofluid, see Figure 21.

The measured and modelled frequency response of the driver on a plane-wave tube are shown in Figure 11. The electrical impedance, which may also be derived, was calculated and is shown in Figure 12.

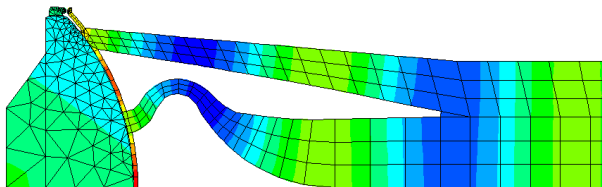


Figure 10

Pressure contour plot of pressure in compression driver and start of plane-wave tube at 13kHz

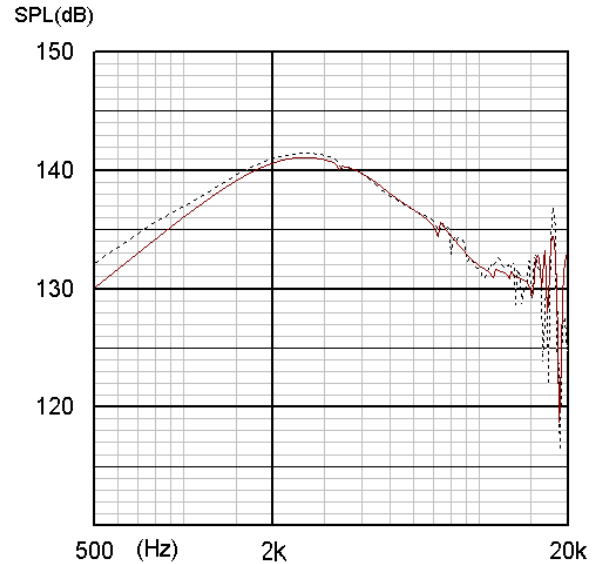


Figure 11

SPL frequency response for real driver (dashed) versus FEM modelled driver (solid) on real and virtual plane-wave tubes

These results are very encouraging; the FEM derived SPL matches the measured results within 1dB from 1kHz to 13kHz. This good match might have been more difficult to achieve in a less "well behaved" driver. It is interesting to note that the model does not predict every mode; perhaps non-axisymmetric modes and spurious structural modes in the tube could be responsible for these features.

The match between real and modelled impedance results is very close. The impedance curve has a maximum value of 12.6 Ohms and a minimum of 6.7 Ohms reflecting the high degree of mechanical damping provided by the driver.

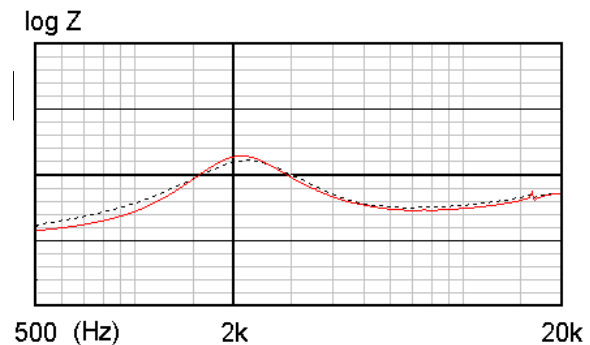


Figure 12

Modulus of electrical input impedance plotted against frequency for real driver (dotted) versus modelled driver (solid)

7. Application of the model.

It now seems instructive to illustrate the design process with some results from example geometries. These are re-worked with the same material values used in the validation presented above. Throughout this paper ‘parametric geometries’ were used enabling many design iterations to take place for little extra cost in time or money. The actual geometry used was a result of about 50 acoustic models and a similar number of magnetic models.

Unlike horns with their various dispersion characteristics, the plane wave tube gives an absolute efficiency of a compression driver. However, we have seen that the high-frequency response is flawed. Consequently, during the driver development, we also modelled the driver on an axisymmetric horn to allow evaluation of the high frequency driver response. While these results are not illustrated here a non-axisymmetric test horn is illustrated and discussed in section 9.

7.1. Phase plug spacing

Firstly, we will look at the effect of doubling the distance between the phase-plug and the diaphragm. This geometric perturbation has been achieved by altering a parameter defining the position of the coordinates of the points associated with the diaphragm. The geometry may then be re-meshed and re-analysed.

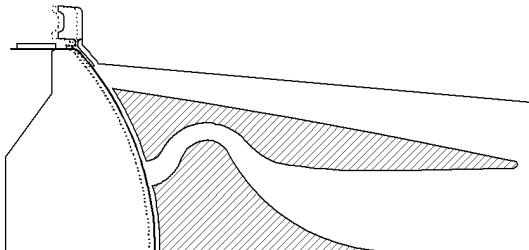


Figure 13

Driver with phase-plug to diaphragm spacing doubled (dotted lines)

The resulting response curve, see Figure 14, shows the decreasing frequency of the HF roll-off, as we would expect from lumped element analysis [8]. However, from the FEM analysis, we can also see changes of magnitude and frequency of some cavity modes. Should we wish to investigate the effect of this change in geometry on, for example, the pressure at any point in the air or the displacement of any part of the structure it is a simple matter to extract the results from the analysis.

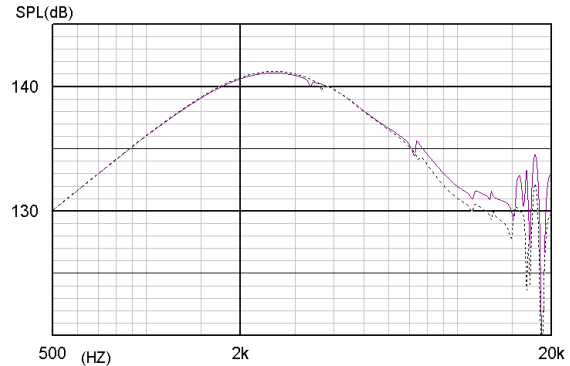


Figure 14

Frequency response of driver with phase-plug to diaphragm spacing doubled (dotted lines)

7.2. Phase-plug inner slot path shape

One of the major features of the design is the use of a curved inner path through the phase plug. The intention of this path is to produce the correct wavefront shape to radiate into a 25 degree conical horn. The straight slot version is illustrated below.

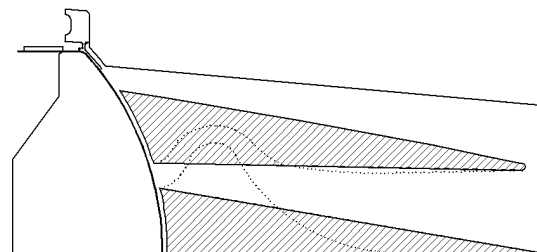


Figure 15

Simplified driver with straight inner slot

As one could expect, the mismatch between the phase-plug slots path length results in a number of severe response dips. These are shown in Figure 16.



Figure 16

Frequency response of driver with straight slots (dotted) compared to reference design (solid)

8. HEAT

For this work, it was decided to produce a static thermal FEM model of the driver with a similar method to that used in previous work [9]. Due to the high frequencies being considered, the omission of forced convection within the driver seems an acceptable simplification. This model was intended to determine the thermal effect of various materials and the effect of including a heat-sink. There was no driver available at the time of analysis, so the results are qualitative rather than absolute.

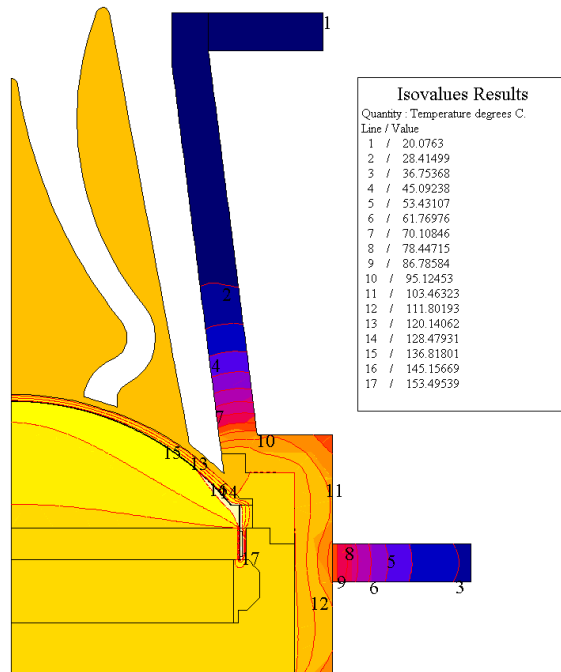


Figure 17

Thermal model of driver showing static temperature contours

The results tabulated in Table 1 are in the form of thermal resistance between coil and environment, together with materials used. It is not surprising to find that the driver with the magnetic fluid, metal components and heat-sink will achieve the coolest coil temperature. We must also take into account that the maximum temperature for a voice coil in air is limited by the wire insulation at around 180 degrees Celsius. For a fluid-filled gap, maximum temperature is limited by the magnetic fluid itself to 120 degrees Celsius.

Rear Heatsink	Diaphragm carrier Material	Dome & Former Material	Magnetic gap fluid	Driver Thermal resistance c/w
yes	Aluminium	Aluminium	ferrofluid	5
yes	ABS	Aluminium	ferrofluid	6
yes	ABS	PETP & Kapton	ferrofluid	6
no	Aluminium	Aluminium	ferrofluid	9
yes	Aluminium	Aluminium	air	10
yes	ABS	Aluminium	air	12
no	ABS	Aluminium	ferrofluid	13
no	Aluminium	Aluminium	air	14
no	ABS	PETP & Kapton	ferrofluid	15
no	ABS	Aluminium	air	18
yes	ABS	PETP & Kapton	air	18
no	ABS	PETP & Kapton	air	27

Table 1

Thermal resistance results from thermal FEM

These results led to the choice of a basic driver with a one-piece aluminium dome, an aluminium diaphragm carrier and a Ferrofluid-filled magnetic gap.

If we consider the effect of temperature rise on the voice coil resistance, we could expect that the driver will not achieve the SPL implied by its sensitivity at high input powers. For a ten watt input we could expect 3dB power compression from the generic front loaded driver with a one-inch diameter coil; the new design suffers from only 1dB of power compression due to the larger coil size and materials chosen.

9. HORN LOADED DRIVER PERFORMANCE.

To evaluate the final compression driver model, a 3D FEM model of a horn was produced. This model was somewhat simplified due to the length of time required to solve 3D problems.

Firstly the two planes of symmetry in the design were used to justify modelling only a quarter of the horn. A further plane of symmetry, in the plane of the horn mouth, was applied to the boundary element to model the 2π baffle.

Secondly, the driver's moving parts were simplified. The dome itself is modelled in 3D semi-loof shell elements. The voice coil, surround and former were modelled as lumped mass, stiffness and damping elements applied to the edge of the dome.

Thirdly, the element size was made somewhat larger than for the axisymmetric model. In particular the circumferential element length has been chosen with the assumption that the wavefront shape is approximately parallel to the mouth profile.

The mesh used for this analysis is illustrated in Figure 18. A parametrically defined geometry was used to create the mesh, in terms of the horn length and cut-off frequencies, of the horizontal and vertical sections. A boundary element is used to model radiation from the finite element modelled fluid within the horn and driver into half-space.

Measurement points may be defined in any position in half-space. For this model, they were defined at a 1m distance from the horn mouth along horizontal and vertical arcs. Directivity plots may be produced from this data and displayed in the usual manner. This data is very useful since no other method of predicting horn directivity exists. For the sake of simplicity, only on axis results have been illustrated here.

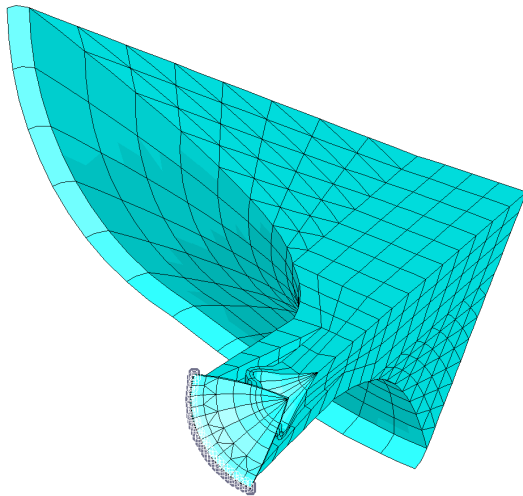


Figure 18
FEM model of horn and driver

The axial response from the model was calculated and is shown in Figure 19 in comparison to a measured compression driver and horn. The match is quite good but is limited at high and low frequencies by the model simplifications mentioned in the previous paragraphs.

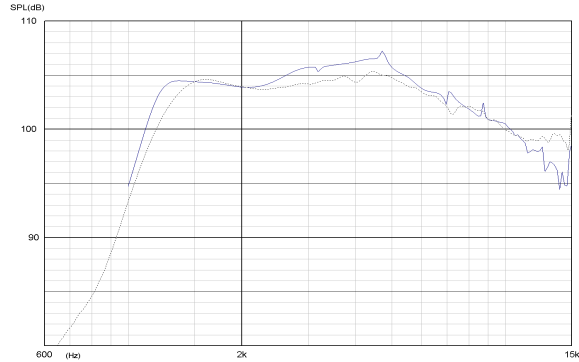


Figure 19
SPL of horn/driver model for 1 meter distance on axis. (solid curve)
Real driver and horn (dotted curve)

To illustrate the 'real world' driver performance on this horn, the driver fundamental and second and third harmonics were measured with a 10W nominal input from 500Hz to 20kHz. These results are shown in Figure 20. For the purposes of comparison the benchmark 'generic front loaded' drivers have been measured under the same conditions. These results are shown in Figure 21.

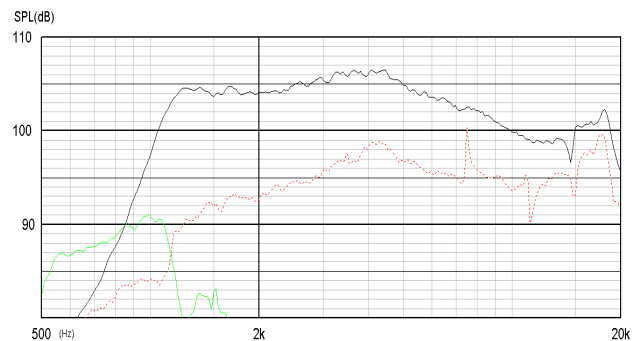


Figure 20
SPL, 2nd 3rd harmonic distortion of final driver at 1m on axis for 10w input on elliptical horn. Distortion raised 20dB

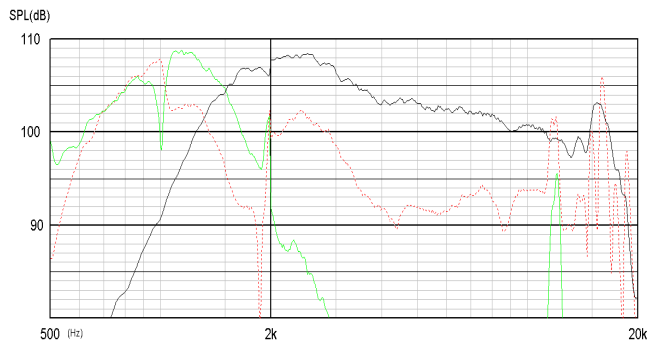


Figure 21
SPL, 2nd 3rd harmonic distortion of 'benchmark' generic driver at 1m on axis for 10w input on elliptical horn. Distortion raised 20dB

10. CONCLUSION

The electro-magneto-vibro-acoustic FEM described in this paper allows the response of electro-dynamic drive units to be calculated without the need to make numerous prototypes. All that is required is the geometry, the material properties and suitable FEM software.

The thermal FEM has significant limitations but produces results with real practical value.

The combination of methods in practice has proved invaluable in the design of a new compression driver.

11. ACKNOWLEDGMENT

I would like to thank the GPAcoustics engineering team for the help and support in writing this paper.

12. REFERENCES

- [1] Dodd, M. A. "A New Compression Drive Unit" IOA Reproduced Sound, conference proceedings 1998.
- [2] Geddes, E. "Computer Simulation of Horn Loaded Compression Driver" JAES, vol.35, No. 7, 1987.
- [3] Smith, B.H. "An Investigation of the Air Chamber of Horn Type Loudspeakers." JASA, vol.25, No. 2, 1953.
- [4] PAFEC FE, "Acoustics Manual" PACSYS Ltd. Strelley Hall, Nottingham UK.
- [5] Dodd, M. A. "The Transient Magnetic Behaviour of Loudspeaker Motors" Presented at the 111th Convention 2001.
- [6] FLUX2D 7.60 User Manual, CEDRAT, Meylan France. 2002.
- [7] Betran, C.I. AES preprint 4787 'Calculated Response of a Compression Driver using a Coupled Field Finite Element Analysis.' September 1998
- [8] Bie, D. "Design and Theory of a New Midrange Horn Driver" Presented at the 93rd Convention 1992.
- [9] Dodd, M. A. "The Application of FEM to the analysis of Loudspeaker Motor Thermal behaviour." Presented at the 112th Convention 2002.